The Eighteenth International Symposium on Artificial Life and Robotics 2013 (AROB 18th '13),
Daejeon Convention Center, Daejeon, Korea, January 30-February 1, 2013

Reduction of Impact when a Humanoid Robot Lands on the Ground

Homare Fujieda, Shingo Okamoto[1], Jae Hoon Lee

Ehime University, Japan
(Tel: 81-89-927-9740, Fax: 81-89-927-9740)

[1]okamoto.shingo.mh@ehime-u.ac.jp

Abstract: The purpose of this research is to reduce the impact force when robot land on the floor by landing motion. First, landing postures of a human were analyzed measuring impacts when the human land on the floor. Through the experimental result on relations between landing postures and the impact forces, it was hypothesized that a human may reduce the impact force by motion control of gravity center of the human, for example to lengthen the time in landing motion. Then a landing robot was developed and the experiment to measure the impact forces was conducted, in order to prove the hypothesis.

Keywords: Humanoid robot, Impact reduction, Passive landing, Active landing, Numerical calculation.

1 INTRODUCTION

Recently, researches about humanoid robots have been well-advanced. In consequence of the well-advance, the humanoid robots became able to practice various motions, such as walking, jumping, and low-speed running. Then, as the development of the humanoid robots is advanced more, the humanoid robots will be needed to behave more intensely for example, like high-speed running. Then, the impact that robots receive in the high-speed running will become a big problem hereafter. This impact may cause various troubles like falling and damage of parts.

The purpose of this research is to reduce the impact when a robot land on the floor by landing motion. Here, we focused on the shifting gravity center of the human in landing on the floor. Then, the experiment to measure the impact was conducted in order to prove that the impact can be reduced by motion control of gravity center of the humanoid robot during landing motion.

2 LANDING OF A HUMAN

2.1 Taking moving images

We took moving images of human's landing by a high-speed camera (CASIO: EX-FH25). Then landing postures when a human lands on the floor was analyzed. Two types of landing, a usual landing and a IR(Impact Reduction)landing, were analyzed. The result of moving images is shown in Figure 1. Through the comparison of two results, it was found that (1) there is no difference between the usual and the IR landing in a touchdown motion and, the human bends his knees more in considering impact reduction than the usual landing. It means that a human shifts slowly down his gravity center when he needs to reduce the impact.

2.2 Measurement of impact

Figure 2 shows the impact force for each landing posture. The period of time from beginning to end of landing motions of the usual and IR landings were 0.480[s] and 0.935[s], respectively. The period of time of IR landing was twice as long as that of usual landing. Then, the impact forces of the usual and IR landings were 2.48×10^3[N] and 1.50×10^3[N], respectively, and that of IR landing decreased by 40 [%] to that of the usual one. From these results, it was hypothesized that a human may reduce the impact by motion control his gravity center, for example, to lengthen the period of time in landing motion.

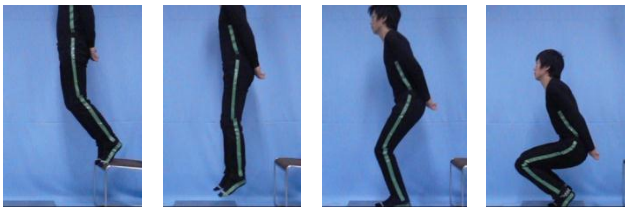

(1) t = 0.00s (2) t = 0.12s (3) t = 0.21s (4) t = 0.39s

(a) Usual landing

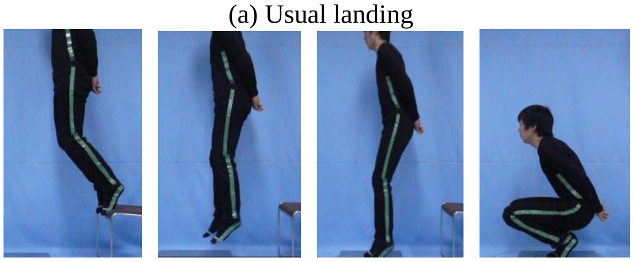

(1) t = 0.00s (2) t = 0.12s (3) t = 0.21s (4) t = 0.43s

(b) IR Landing

Fig. 1. Moving images of human's landing

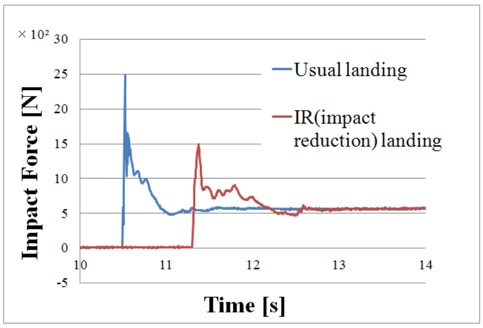

Fig. 2. Impact forces to variable landing postures

3 CONPUTATIONAL CALCULATION

3.1 Analysis model

An analysis model of a landing robot was designed and the numerical calculation was performed in order to develop the landing robot. Figure 3 shows the analysis model of a landing robot. The analysis model is composed of a foot, an upper body, a shin and a thigh.

The landing robot falls along a rail with a slope in order to diminish the speed in shifting gravity center of the robot so that a motor can control its speed. Then the physical parameters of the lengths, the masses, the inertia moments, the coefficient of viscosity and the spring constant used in the calculation are shown in Table 1.

3.2. Equation of motion

The equation of motion is given by

$$\boldsymbol{M\ddot{Q}} + \boldsymbol{C\dot{Q}} + \boldsymbol{KQ} = \boldsymbol{\tau} - \boldsymbol{G} \tag{1}$$

where $\boldsymbol{Q} = \{u_1 \quad \theta\}^T$, $\boldsymbol{\tau} = \{0 \quad \tau_1\}^T$, $\boldsymbol{M}$ is a inertia matrix, $\boldsymbol{C}$ is a damping matrix, $\boldsymbol{K}$ is a stiffness matrix and $\boldsymbol{G}$ is a gravity vector. The components of matrixes and vector in Eq.(1) are represented as

$$\boldsymbol{M} = \begin{bmatrix} M_{11} & M_{12} \\ M_{21} & M_{21} \end{bmatrix}, \tag{2}$$

where

$$M_{11} = m_1 + m_2 + M_1 + M_2, \tag{3}$$

$$M_{12} = -\{(m_1 + m_2)(L_1 + L_2) + M_1 l_1 - M_2 l_2\} \sin\theta, \tag{4}$$

$$M_{21} = -\{(m_1 + m_2)(L_1 + L_2) + M_1 l_1 - M_2 l_2\} \sin\theta, \tag{5}$$

$$M_{22} = \{(m_2 + M_2)(L_1 + L_2)^2 - 2M_2 l_2 (L_1 + L_2)\} sin^2\theta + M_1 {l_1}^2 + M_2 {l_2}^2 + J_1 + J_2, \tag{6}$$

$$\boldsymbol{C} = \begin{bmatrix} C_{11} & C_{12} \\ C_{21} & C_{22} \end{bmatrix}, \tag{7}$$

where

$$C_{11} = C_f, \tag{8}$$

$$C_{12} = -\{(m_1 + m_2)(L_1 + L_2) + M_1 l_1 - M_2 l_2\}\dot{\theta} \cos\theta, \tag{9}$$

$$C_{21} = 0, \tag{10}$$

$$C_{22} = 0.5\{(m_2 + M_2)(L_1 + L_2)^2 - 2M_2 l_2 (L_1 + L_2)\}\dot{\theta} sin2\theta + 4c_j, \tag{11}$$

$$\boldsymbol{K} = \begin{bmatrix} K_{11} & K_{12} \\ K_{21} & K_{22} \end{bmatrix}, \tag{12}$$

where

$$K_{11} = k_f, \tag{13}$$

$$K_{12} = 0, \tag{14}$$

$$K_{21} = 0, \tag{15}$$

$$K_{22} = 4k_j, \tag{16}$$

$$\boldsymbol{G} = \{G_1 \quad G_2\}^T, \tag{17}$$

where

$$G_1 = (m_1 + m_2 + M_1 + M_2) g \sin\alpha, \tag{18}$$

$$G_2 = -\{(m_1 + m_2)(L_1 + L_2) + M_1 l_1 - M_2 l_2\} g \sin\theta \sin\alpha + (M_1 l_1 + M_2 l_2) g \cos\theta \cos\alpha - 2k_j(\pi - \theta_0), \tag{19}$$

3.3. Passive landing

3.3.1 Calculation method

A computer simulation using the Newmark-β method was performed in a numerical calculation, and Scilab was used as a computer language. Then control torque τ_1 was set at zero in this calculation. The spring constant k_f was given as Eq.(20). These parameters were decided based on the experiment. Then the coefficient of velocity c_f was given as Eq.(3).

$$k_f = 267{,}459(u_1 - h_1 - 0.08)^2 - 1{,}790.1(u_1 - h_1 - 0.08), \tag{20}$$

$$c_f = \beta_2 k_f, \tag{21}$$

The values of β_1 and β_2 were set at 5.15×10^{-2} and 7.50×10^{-1}, respectively. The initial height of the landing robot was set at 0.3[m].

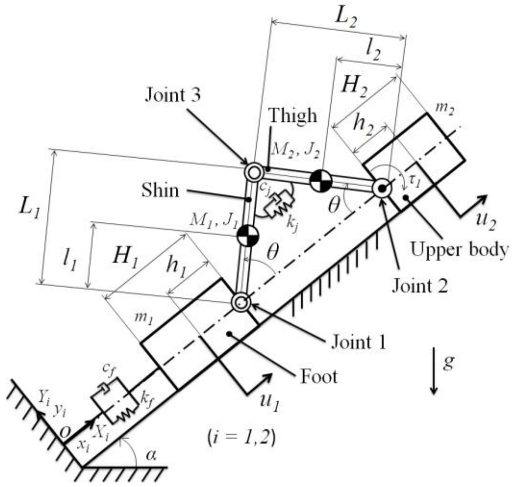

H_1 : Length of the foot, H_2 : Length of the upper body
L_1 : Length of the shin, L_2 : Length of the thigh
h_1 : Length from the joint 1 to the gravity center of the foot
h_2 : Length from the joint 2 to the gravity center of the upper body
l_1 : Length from the joint 1 to the gravity center of the shin
l_2 : Length from the joint 2 to the gravity center of the thigh
m_1 : Mass of the foot, m_2 : Mass of the body
M_1 : Mass of the shin, M_2 : Mass of the thigh
J_1 : Inertia moment of the shin, J_2 : Inertia moment of the thigh
k_j : Spring constant of the joint 3
c_j : Coefficient of viscosity of the joint 3
k_f : Spring constant of the foot
c_f : Coefficient of viscosity of the foot
θ : Rotation angle of the shin(or thigh)
u_1 : Displacement of the foot, u_2 : Displacement of the upper body
τ_1 : Control torque, α : Angle of the slope

Fig. 3. Analysis model of the landing robot

Table 1. Physical parameters of analysis model

m_1 [kg]	2.40	L_1 [m]	2.10×10^{-1}
m_2 [kg]	1.56	L_2 [m]	2.10×10^{-1}
M_1 [kg]	3.10×10^{-1}	l_1 [m]	1.05×10^{-1}
M_2 [kg]	3.10×10^{-1}	l_2 [m]	1.05×10^{-1}
H_1 [m]	1.70×10^{-1}	J_1 [kg•m^2]	2.11×10^{-3}
H_2 [m]	8.00×10^{-2}	J_2 [kg•m^2]	2.11×10^{-3}
h_1 [m]	8.50×10^{-2}	c_j [kg/m•s]	$\beta_1 k_j$
h_2 [m]	4.00×10^{-2}	k_j [kg•m^2/s^2•rad]	3.20

3.3.2 Calculated results

Figure 4 shows the time histories of u_1 and u_2. The experiment of the landing robot was conducted based on this result.

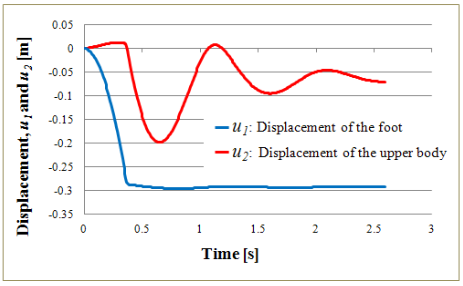

Fig. 4. The calculated time histories of u_1 and u_2 in passive landing

3.4 Active landing

3.4.2 Calculation method

Two types of control method, the proportional control and the proportional-differential control were used. Then the spring constant of the joint 3 k_l and coefficient of viscosity of the joint 3 c_l were set at zero in this calculation.

3.4.3 P control (Proportional control)

The block diagram of an active control for calculation is shown in Figure 5. The control torque τ_1 loaded to the upper body was given by Eq.(22) when the proportional control was used.

$$\tau_1 = k_p(\theta_d - \theta) \qquad (22)$$

The calculated result of the proportional control is shown in Fig. 6 when setting at the control gain k_p = 200[N•m/rad], the desired angle of the shin(or thigh) θ_d = 87[deg], and the angle of the shin(or thigh) θ = 87[deg] corresponding to the displacement of the upper body u_2 = 0.2[m]. Then control gain k_d was set at zero in this calculation.

3.4.4 PD control (Proportional-differential control)

The block diagram of an active control for calculation is shown in Figure 5. The control torque τ_1 loaded to the upper body was given by Eq.(23) when the PD control is used. The k_p and k_d denote the control gain.

$$\tau_1 = k_p(\theta_d - \theta) + k_d(\dot{\theta}_d - \dot{\theta}) \qquad (23)$$

The calculated result of the PD control is shown in Fig. 6 when setting at the control gain k_p = 200[N•m/rad], the desired angle of the shin(or thigh) θ_d = 87[deg], the desired angular velocity of the shin(or thigh) $\dot{\theta}_d$ = 0[m/s].

3.3.2 Calculated results

Figure 6 shows the comparison of the displacement u_2 of the upper body between the proportional and the PD controls. It was found that the displacement u_2 was stabilized by using the PD control.

4 DESIGN AND DEVELOPMENT OF EXPERIMENTAL SET-UP

4.1. Landing robot

Figure 7 shows a landing robot. The landing robot is composed of a foot, an upper body, the shin and the thigh. Two rotary encoders are installed to measure the rotation angles. The displacement of the foot and the upper body are calculated by them. The torsion springs are attached to the knee joint to connect the shin and the thigh, in order to give a spring effect that thigh muscles of a human generate.

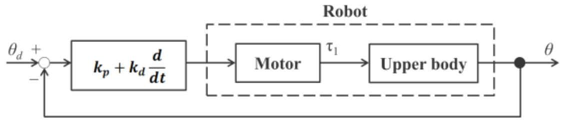

k_d = 0 : P control, $k_d \neq$ 0 : PD control

Fig. 5. Block diagram of an active control for calculation

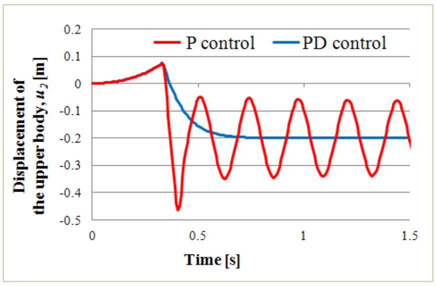

Fig. 6. Comparison of the displacement u_2 of the upper body between the proportional and the proportional-differential controls

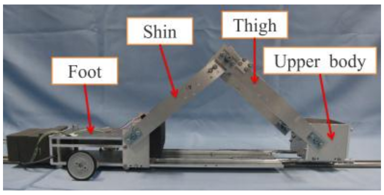

Fig. 7. Landing robot

Fig. 8. Guide flame with a slope

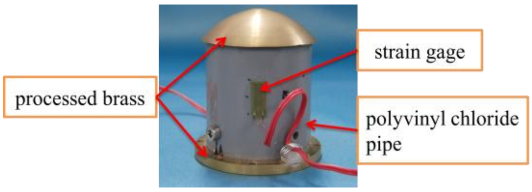

Fig. 9. Force sensor

4.2. Guide flame with a slope

Figure 8 shows a guide flame with a slope. This slope angle can be changed to desired angle. A rail that the landing robot falls along the slope is attached on the guide flame.

4.3. Force sensor

A force sensor to measure the impact which the landing robot is subjected to was developed. Figure 9 shows the force sensor. The force sensor is composed of a polyvinyl chloride pipe, parts of processed brass and strain gages.

5 EXPERIMENT OF THE LANDING ROBOT

5.1. Passive landing

5.1.1 Experimental method

The initial angle of the shin(or the thigh) was set at θ = 45[deg], and initial height of the landing robot at 0.3[m]. The spring constant of the torsional spring was set at 4.62[kg•m²/s²•rad]. The experiment was conducted in two types of landing condition, (a)a landing with shifting gravity center of the robot and (b)a landing with fixing the distance between the foot and the upper body. Then both the impact forces when the robot lands on the ground and the positions of the moving body were measured to each condition.

5.1.2 Experimental results

Figure 10 shows the impact force on each condition. Figure 11 shows the comparison of u_1 and u_2 between calculation and experimental result. The period of time from beginning to end of landing motions of the (a) and (b) were 0.095[s] and 0.073[s], respectively. The period of time of (a) was 1.3 times as long as that of (b). Then the impact forces of (a) and (b) were 2.84×10^2[N] and 5.81×10^2[N], respectively, and that of (a) decreased by 50 [%] to that of (b). It was found that the impact force when the robot lands on the ground can be reduced by shifting gravity center of the robot. Then the displacement of the foot u_1 and the upper body u_2 in the experiment follow the displacement in calculation. As this result, a validity of the landing robot was confirmed.

5.2. Active landing

5.2.1 Installation of a motor

A motor was installed at the upper body to reproduce effect of the torsion spring. The landing robot installed the motor as shown in Figure 12.

5.2.2 Control method of the motor

The PD control was used for control of the motor. The block diagram of an active control for landing robot is shown in Figure 5. The desired angle θ_d of the shin(or thigh) and the desired angular velocity $\dot{\theta}_d$ of the shin(or thigh) was set at 87[deg] and zero, respectively.

5.2.3 Experimental method

The motor is controlled using the conditions gotten in the experiment. Then both the impact forces when the robot lands on the ground and the positions of the moving upper body are measured, and the control gains so that the motor can reproduce the effect of torsion spring are examined.

5.2.4 Experimental results

The experiment has been being conducted currently.

6 CONCLUSION

The way to reduce the impact when the robot lands on the ground had been studied. The summaries of the results are:

(1) It was hypothesized that a human may reduce the impact by motion control of his gravity center, for example, to lengthen the period of time in landing motion.

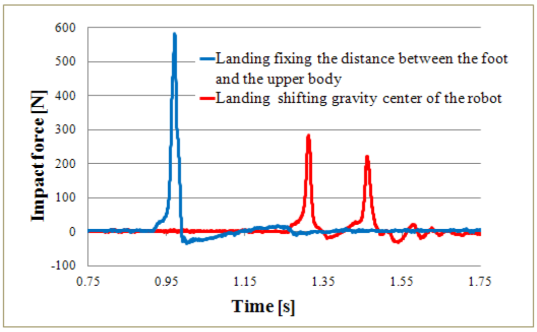

Fig. 10. Impact forces to each condition

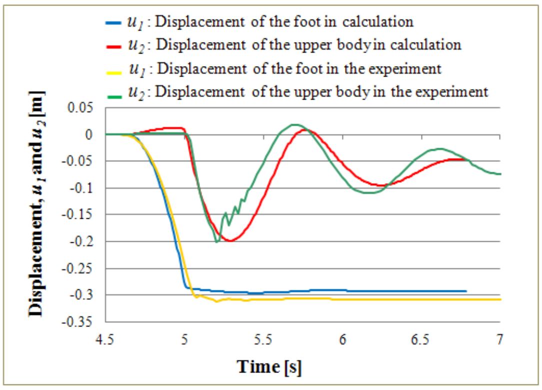

Fig. 11. Comparison of u_1 and u_2 between calculation and experimental result in the passive landing

Fig. 12. The landing robot installed the motor

(2) The analysis model of the landing robot was designed and the control gains k_p and k_d were found in the computational calculation.

(3) The landing robot was designed and developed considering the calculated results.

(4) The experiment of the landing robot with passive landing was conducted. Then the effect of shifting gravity center of the robot in landing motion was confirmed.

The experiment of the landing robot with active landing has been being conducted. For the future, it will be proved that the impact when the robot lands on the ground is reduced by motion control of the robot through the experimental results.

REFERENCES

[1] Tazaki T, Tomita M, Natori T, Shibata M(2002) : Landing impact force reduction on redundant leg biped robot by center of gravity control, vol. IIC-02, no. 15, pp. 1-6